International Journal of Engineering Research & Science (IJOER)
ISSN: [2395-6992]
[Vol-12, Issue-10, October - 2026]
Website: www.ijoer.com
Journal DOI: 10.25125/engineering-journal

Analysis of Thermo-Hydraulic Behavior of a Compact Heat Exchanger with TPMS Structures

Romana Dobáková[1*]; Peter Milenovský[2]; Daniel Kóňa[3]

Department of Power Engineering, Faculty of Mechanical Engineering, Technical University of Košice, 04200 Košice, Slovakia
*Corresponding Author

Received: 24 September 2026/ Revised: 03 October 2026/ Accepted: 15 October 2026/ Published: 31-10-2026
Copyright @ 2026 International Journal of Engineering Research and Science
This is an Open-Access article distributed under the terms of the Creative Commons Attribution Non-Commercial License (https://creativecommons.org/licenses/by-nc/4.0) which permits unrestricted Non-commercial use, distribution, and reproduction in any medium, provided the original work is properly cited.

Abstract— *This paper presents the design and numerical evaluation of a compact heat exchanger employing TPMS (Triply Periodic Minimal Surfaces) structures. Attention is focused on the characteristics of selected TPMS structures, their implementation in the heat exchanger design, and the selection of a suitable geometric configuration in terms of thermal performance and pressure losses. The heat exchanger geometry was designed in Creo Parametric, while the TPMS structures themselves were generated using nTop software. Their thermo-hydraulic properties were evaluated by numerical simulations in ANSYS CFX, focusing on the influence of geometric and operating parameters. Based on the numerical simulation results, the most suitable variant was selected as a compromise between the achieved thermal performance and hydraulic losses.*

Keywords— TPMS, additive manufacturing, ANSYS CFX, heat exchanger.

I. INTRODUCTION

Heat exchangers are an important component of many technological and energy systems, where they provide the transfer of thermal energy between two or more media. Their structural arrangement significantly affects heat-transfer intensity, pressure losses, dimensions, and the overall efficiency of the device. Therefore, when designing modern heat exchangers, it is important to identify geometric solutions that enable efficient use of the available space while maintaining favorable thermal and hydraulic characteristics.

One promising approach to the design of compact heat exchangers is the use of TPMS (Triply Periodic Minimal Surfaces) structures. This is a design concept in which the geometry repeats in three spatial directions and is characterized by zero mean curvature. Their specific geometry makes it possible to create complex, interconnected three-dimensional channels with a high ratio of heat-transfer area to the total volume of the device, thereby providing favorable conditions for heat-transfer intensification while minimizing the space required for installation of the device.

When TPMS structures are applied in heat exchangers, the available heat-transfer area increases substantially compared with conventional geometric solutions. The complex nature of the flow within the structure also promotes fluid mixing and disruption of the thermal boundary layer, which may increase the heat-transfer coefficient. Another advantage of TPMS structures is the possibility of parametric control of their geometry, for example through the unit-cell size, relative density, or wall thickness. By varying these parameters, both the thermal and hydraulic characteristics of the resulting structure can be modified. The use of TPMS structures in heat exchangers is also closely associated with the development of additive manufacturing technologies. These technologies enable the fabrication of geometrically complex structures that could be produced by conventional manufacturing processes only with substantial limitations.

II. CHARACTERISTICS OF TPMS STRUCTURES

The basic elements of TPMS geometry are three-dimensional geometric structures characterized by specific properties. The characteristic geometric element of TPMS structures is a surface whose mean curvature is zero at every point. Such a surface

locally minimizes its area within a given boundary. TPMS structures can form highly complex spatial geometries and, when suitably arranged, enable the formation of continuous channels and a large surface area relative to volume. Mathematically, the minimal surface characteristic of TPMS structures with zero mean curvature is given by [1]:

$$H = \frac{k_1 + k_2}{2} = 0 \quad (1)$$

where H is the mean curvature of the surface, and k_1 and k_2 are the principal curvatures at the given point. The condition H = 0 means that the principal curvatures at each point have equal magnitudes and opposite signs.

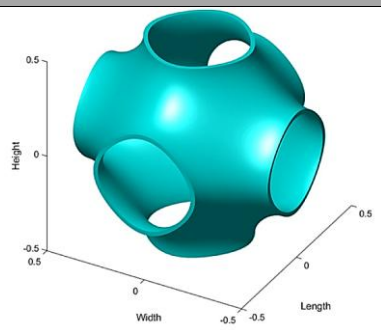
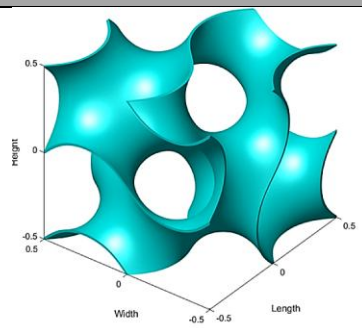
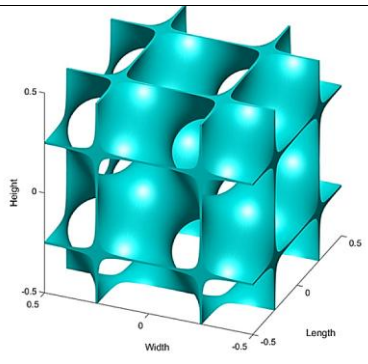
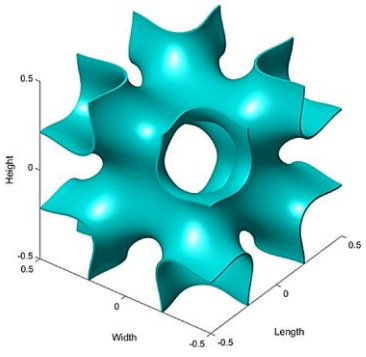
A specific group of TPMS structures consists of periodic structures in which the geometry repeats in space. If periodicity occurs in three mutually perpendicular directions, the structures are referred to as triply periodic, i.e., TPMS. Owing to their spatial geometry, they provide a high surface-area-to-volume ratio and form continuous, interconnected domains suitable for the passage of a flowing medium. Their geometry is defined by an implicit function of three spatial coordinates, and the resulting surface is obtained by specifying an isosurface for a particular function value. In general, the implicit representation of a TPMS can be written in the form [2]:

$$f(x, y, z) = C \quad (2)$$

where C represents a constant value defining a specific function level, and x, y, z are the spatial coordinates. Changing the value of C shifts the resulting isosurface, thereby changing the volume ratio of the separated channels and the relative density of the structure with respect to the reference minimal surface (C = 0).

Commonly used types of TPMS structures include Schwarz Primitive (P), Schwarz Diamond (D), Schoen Gyroid (G), and Schoen I-WP (IWP). The individual types differ in their topology and in the character of the channels they form, which affects their hydraulic and thermal properties. The selection of a specific geometry therefore represents an important parameter in heat-exchanger design. A basic visualization and comparison of these structures is provided in Table 1.

TABLE 1
SELECTED TPMS TYPES AND THEIR VISUALIZATION [3]

Minimal Surface	3D View	Minimal Surface	3D View
Schwarz Primitive		Schoen Gyroid	
Schwarz Diamond		Schoen I-WP	

For practical application, however, their thermo-hydraulic behavior under real operating conditions must be assessed using simulation tools that couple fluid flow and heat transfer.

III. STRUCTURAL DESIGN OF A COMPACT HEAT EXCHANGER BASED ON TPMS STRUCTURES

An important characteristic of heat exchangers designed using TPMS structures is the interdependence between thermal performance and pressure losses. More complex geometry and more intensive mixing of the flowing medium may enhance heat transfer, but at the same time may cause higher hydraulic losses. Therefore, the design of a suitable TPMS geometry requires evaluation of both characteristics and identification of an appropriate compromise between thermal performance and an acceptable pressure drop.

The heat exchanger model was created in Creo Parametric. A cylindrical shape was selected, with inlet and outlet ports and an internal space intended for the creation of the TPMS structure. The external length of the heat exchanger body was designed to be 98 mm and its external diameter 50 mm. The internal diameter of the main part of the heat exchanger was 46 mm. The inlet and outlet ports were designed with G 1/4 threads. The transition between the cylindrical part of the body and the end sections of the heat exchanger was formed by beveled surfaces at an angle of 135°. This shape provides a more uniform pressure distribution, smoother fluid flow, and easier modification of the model. The model was subsequently exported in STEP format for further processing in nTop software.

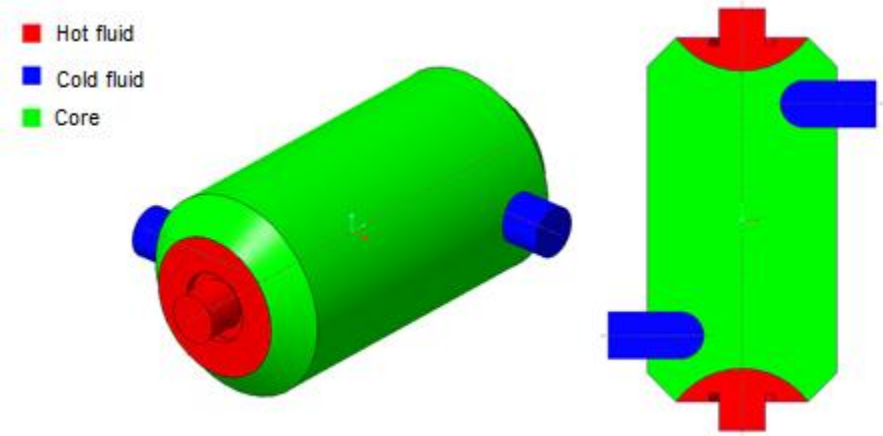


FIGURE 1: 3D model of the heat exchanger without a TPMS structure in Creo Parametric

nTop software was selected because of its ability to efficiently model geometrically complex TPMS structures, whose creation is significantly limited in conventional CAD software. It enables the creation of an implicit heat exchanger model and the generation of TPMS structures, allowing their shape and size to be easily modified without altering the basic geometry created in Creo Parametric. This approach enables rapid generation of design variants suitable for numerical analysis [4, 5]. The final heat exchanger model was exported from nTop in the required format to the software used for numerical simulations of fluid flow and heat transfer.

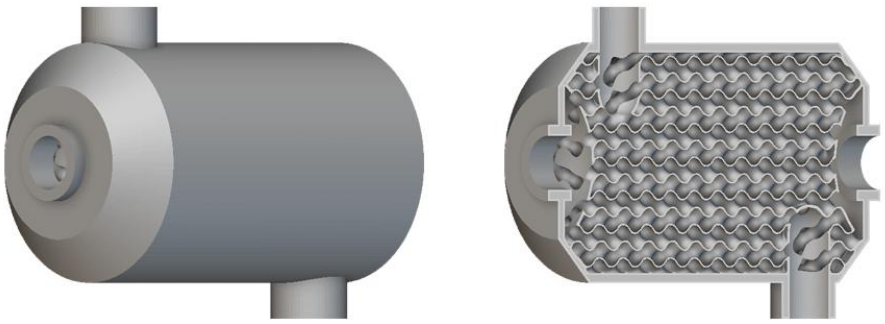
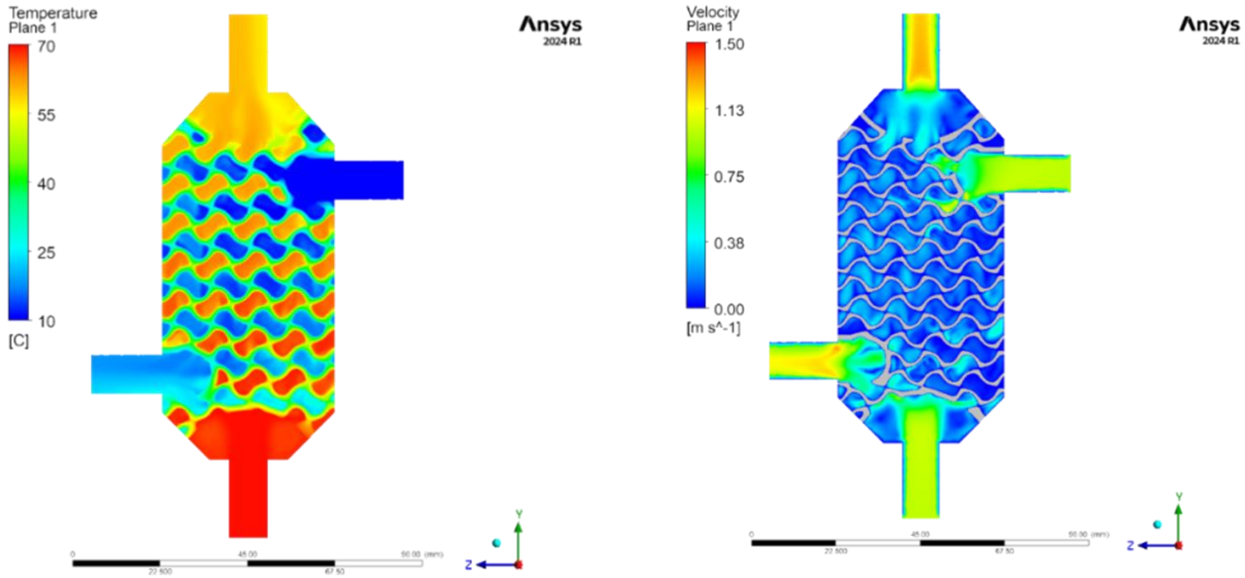


FIGURE 2: Final 3D model of the heat exchanger with a TPMS structure in nTop

Performing a numerical analysis of heat transfer and fluid flow in ANSYS CFX was essential to verify the functionality of the heat exchanger with TPMS structures prior to additive manufacturing and experimental testing. Simulations in this software tool enable detailed analysis of the behavior of the working medium, including changes in its velocity, pressure, and

temperature, even in regions that are difficult to access during real measurements. The ability to readily compare different geometric variants, materials, or operating conditions makes it possible to accurately assess the influence of the internal structure on heat-transfer intensity, flow behavior, and the magnitude of hydraulic losses.

For the numerical simulations, a heat exchanger with a gyroid TPMS geometry was selected (cell size 10 mm, wall thickness 1 mm, and total heat exchanger length 98 mm). The inlet flow parameters were defined by a hot-water inlet temperature of 70 °C and a cold-water inlet temperature of 10 °C. At a flow velocity of 1 $m \cdot s^{-1}$ and an inlet-port diameter of 11.4 mm, the volumetric flow rate corresponded to 6.12 $l \cdot min^{-1}$. The inlets and outlets were configured so that the media flowed in a counter-current arrangement. After the geometry and computational mesh had been created, the boundary conditions and material properties were defined in ANSYS CFX. Water was specified as the flowing medium on both the hot and cold sides. The heat exchanger walls were defined using the properties of additively manufactured (solidified) titanium. The results of the simulation of the heat exchanger with gyroid geometry in ANSYS CFX are shown in Fig. 3.



(a) temperature distribution **(b) velocity distribution**

FIGURE 3: Simulation results of a heat exchanger with gyroid geometry in ANSYS CFX

Figure 3a shows, in the central part of the geometry, the distribution of the cooling and cooled liquid regions as they flow through the internal structure. The velocity-field distribution in the section plane is shown in Fig. 3b, where the color scale represents the flow velocity in $m \cdot s^{-1}$, with a maximum value of approximately 1.53 $m \cdot s^{-1}$. The highest velocity values occur at the inlet and outlet ports, which, in accordance with the continuity equation, results from their smaller cross-sectional area compared with the heat-exchanger core. In the central part of the model, the velocity field is markedly nonuniform, which is a direct consequence of the presence of the TPMS structure.

TABLE 2

RESULTS OF THE NUMERICAL SIMULATION IN ANSYS CFX

Parameter	Symbol	Value
Cold water inlet temperature	$t_{c,in}$ (°C)	10
Hot water inlet temperature	$t_{h,in}$ (°C)	70
Cold water outlet temperature	$t_{c,out}$ (°C)	20.37
Hot water outlet temperature	$t_{h,out}$ (°C)	58.83
Cold water temperature difference between inlet and outlet	Δt_c (°C)	10.37
Hot water temperature difference between inlet and outlet	Δt_h (°C)	11.17
Cold side pressure drop	Δp_c (Pa)	1223
Hot side pressure drop	Δp_h (Pa)	1040

Based on the results obtained from the numerical simulation presented in Table 2, the hydraulic power required to overcome the pressure drop could be determined:

$$P_{\mathrm{hydr,c}} = \Delta p_{\mathrm{c}} \cdot Q_v = 1223 \cdot 0.000102 = \ 0.125 \text{ W} \tag{3}$$

$$P_{\mathrm{hydr,h}} = \Delta p_{\mathrm{h}} \cdot Q_v = 1040 \cdot 0.000102 = \ 0.106 \text{ W} \tag{4}$$

where $P_{hydr,h}$ is the hydraulic power on the hot side of the heat exchanger (W), $P_{hydr,c}$ is the hydraulic power on the cold side of the heat exchanger (W), and Q_v is the volumetric flow rate of water ($m^3 \cdot s^{-1}$).

The power required to overcome the pressure drop is minimal; therefore, this pressure drop can be considered very small.

The physical properties of water used in the calculations were considered at its mean temperature (Table 3). The mean temperature was determined as the arithmetic mean of the inlet and outlet temperatures of the respective medium. Based on the temperature determined in this way, the density and specific heat capacity values were obtained from the basic properties of water and subsequently used in the calculation of thermal power and other heat-exchanger characteristics [6, 7].

TABLE 3
PHYSICAL PROPERTIES OF WATER AT THE MEAN TEMPERATURE

Parameter	Symbol	Value
Mean hot water temperature	$t_{\mathrm{h,m}}$ (°C)	64.42
Mean cold water temperature	$t_{\mathrm{c,m}}$ (°C)	15.19
Water density at the mean hot water temperature	ρ_{h} ($kg \cdot m^{-3}$)	980.5
Water density at the mean cold water temperature	ρ_{c} ($kg \cdot m^{-3}$)	998.9
Specific heat capacity at the mean hot water temperature	$c_{\mathrm{p,h}}$ ($J \cdot kg^{-1} \cdot K^{-1}$)	4 183.9
Specific heat capacity at the mean cold water temperature	$c_{\mathrm{p,c}}$ ($J \cdot kg^{-1} \cdot K^{-1}$)	4 186.8

These parameters were subsequently used to calculate the thermal power on the hot and cold sides of the heat exchanger (P_h and P_c) according to the following relationships:

$$P_{\mathrm{h}} = \rho_{\mathrm{h}} \cdot Q_v \cdot c_{\mathrm{p,h}} \cdot \left(t_{\mathrm{h,in}} - t_{\mathrm{h,out}}\right) = 980.5 \cdot 0.000102 \cdot 4183.9 \cdot (70 - 58.83) = 4\,673.9 \text{ W} \tag{5}$$

$$P_{\mathrm{c}} = \rho_{\mathrm{c}} \cdot Q_v \cdot c_{\mathrm{p,c}} \cdot \left(t_{\mathrm{c,out}} - t_{\mathrm{c,in}}\right) = 998.9 \cdot 0.000102 \cdot 4186.8 \cdot (20.37 - 10) = 4\,423.7 \text{ W} \tag{6}$$

From the standpoint of the law of conservation of energy, the thermal powers on the hot and cold sides should theoretically be equal. In the calculation, the physical properties of water were evaluated at the mean temperature of the medium. It is precisely this simplification that causes the minor discrepancy between the calculated thermal outputs. Given the narrow temperature range, however, this deviation is negligible.

After evaluation of the heat balance, the heat-exchanger effectiveness ε was determined:

$$\varepsilon = \frac{P_{\mathrm{ac}}}{P_{\mathrm{max}}} = \frac{\frac{P_{\mathrm{h}}+P_{\mathrm{c}}}{2}}{P_{\mathrm{max}}} \frac{4548.8}{25\,360.4} = 0.179 \tag{7}$$

where P_{ac} is the actual thermal power of the heat exchanger (W), P_{max} is the maximum theoretically possible thermal power of the heat exchanger (W), and is determined from the relationship:

$$P_{\mathrm{max}} = \rho_{\mathrm{ave}} \cdot Q_v \cdot c_{\mathrm{ave}} \cdot \left(t_{\mathrm{h,in}} - t_{\mathrm{c,in}}\right) = 988.8 \cdot 0.000102 \cdot 4190.8 \cdot (70 - 10) = \ 25\,360.4 \text{ W} \tag{8}$$

where ρ_{ave} is the mean value of water density at the average water temperature in the heat exchanger, and c_{ave} is the mean value of the specific heat capacity of water at the average water temperature in the heat exchanger ($J \cdot kg^{-1} \cdot K^{-1}$).

The heat-transfer coefficient k was calculated from Eq. (9); the heat-transfer area was determined using nTop software (S = 0.040727 m^2):

$$k = \frac{P_{\mathrm{ac}}}{S \cdot \Delta T_{\mathrm{m}}} = \frac{4\,548.8}{0{,}040727 \cdot 49.23} = 2268.7 \text{ W} \cdot m^{-2} \cdot K^{-1} \sim 2\,270 \text{ W} \cdot m^{-2} \cdot K^{-1} \tag{9}$$

where:

$$\Delta T_{\mathrm{m}} = \frac{(t_{\mathrm{h,in}} - t_{\mathrm{c,out}}) - (t_{\mathrm{h,out}} - t_{\mathrm{c,in}})}{\ln \frac{t_{\mathrm{h,in}} - t_{\mathrm{c,out}}}{t_{\mathrm{h,out}} - t_{\mathrm{c,in}}}} \quad (10)$$

An analogous procedure was used to evaluate the remaining design variants of the heat exchanger. Using the above relationships, Gyroid structures (G) with wall thicknesses of 0.5 mm and 0.7 mm (cell size 10 mm), Gyroid structures (G) with cell sizes of 7 mm and 12 mm (wall thickness 1 mm), as well as variants with Schwarz (P) and Diamond (D) TPMS structures were evaluated. Flow velocities ranging from 0.25 m·s^{-1} to 1.5 m·s^{-1} were selected, corresponding to flow rates from 1.53 l·min^{-1} to 9.18 l·min^{-1}.

TABLE 4

RESULTS OF NUMERICAL SIMULATIONS OF THE SELECTED TPMS STRUCTURES

Variant	v (m·s^{-1})	Δp_h (Pa)	Δp_c (Pa)	P_{ac} (W)	ε (1)	k (W·m^{-2}·K^{-1})	Δt_h (°C)	Δt_c (°C)
Gyroid 1 mm, 10 mm	0.25	80	78	2257	0.356	1435	21.85	20.87
	0.5	277	269	3319	0.262	1839	16.11	15.29
	1	1040	1223	4548.8	0.179	2270	11.17	10.37
	1.5	2188	2073	5527	0.145	2646	9.09	8.34
Gyroid 0.7 mm, 10 mm	0.25	143	95	2212	0.358	1944	27.65	25.45
	0.5	329	136	3905	0.354	2299	19.84	18.51
	1	930	880	6159	0.206	2586	13.09	12.27
	1.5	1856	1320	6607	0.177	3225	10.68	10.51
Gyroid 0.5 mm, 10 mm	0.25	161	114	2587	0.559	2216	29.86	27.35
	0.5	353	287	4330	0.315	2720	21.78	20.53
	1	1108	985	6525	0.269	3279	14.57	13.85
	1.5	2256	1605	7137	0.209	3804	12	11.98
Gyroid 1 mm, 7 mm	0.25	129	93	3986	0.563	1967	33.02	32.67
	0.5	390	360	4178	0.418	2203	25.06	24.44
	1	1374	1695	6367	0.264	2668	17.23	16.29
	1.5	2820	2411	7612	0.251	3603	13.99	14.09
Gyroid 1 mm, 12 mm	0.25	143	115	2380	0.47	1913	22.63	23.54
	0.5	331	229	3071	0.298	2764	17.17	17.77
	1	1059	1196	4442	0.225	3062	12.11	11.7
	1.5	1917	1684	7228	0.155	3262	9.94	10.37
Schwarz	0.25	230	256	1487	0.35	1290	16.53	16.68
	0.5	620	341	3121	0.191	2915	12.88	13.04
	1	2010	1815	3674	0.166	2748	9.01	8.65
	1.5	3905	3353	5065	0.104	2753	7.55	7.91
Diamond	0.25	172	71	3394	0.452	1801	27.57	28.43
	0.5	403	204	4953	0.306	2140	22.09	23
	1	1413	1313	5783	0.255	2959	15.28	15.11
	1.5	2249	1803	6328	0.227	3443	12.64	13.62

Based on the numerical simulation results, several geometric variants of the TPMS heat exchanger were analyzed. The evaluated parameters were primarily pressure losses on both sides of the heat exchanger, transferred thermal power, heat-

exchanger effectiveness, and the heat-transfer coefficient. The criterion for selecting the optimal geometry was not merely to achieve the maximum thermal power, but to identify a suitable compromise between heat-transfer intensity and the energy required for fluid flow.

Figure 4 presents a graphical comparison of the change in pressure drop Δp_h and the temperature change Δt_h on the cooled side as a function of the fluid inlet velocity to the heat exchanger. It can be observed that reducing the wall thickness of the TPMS structure has a more significant impact on temperature change at lower flow velocities; however, this difference diminishes as the velocity increases. Conversely, the pressure drop exhibits negligible differences at lower velocities, but the variance in pressure drop increases significantly with higher velocities. At higher flow velocities, the configuration with the thinnest wall (0.5 mm) exhibits the highest pressure drop, whereas the variant with the intermediate wall thickness (0.7 mm) demonstrates the lowest pressure drop. The observed pressure-drop behavior at higher flow velocities can be interpreted as a consequence of the interaction between the available flow cross-sectional area and local hydrodynamic effects within the TPMS structure. The differences in hydraulic losses between the variants with wall thicknesses of 0.5 mm and 1.0 mm are likely related to differences in the arrangement of the flow paths and in local flow velocities. For the 1.0 mm wall-thickness variant, the smaller available flow cross-section may lead to higher local flow acceleration and an increase in hydraulic resistance. In contrast, the greater porosity of the 0.5 mm wall-thickness variant may alter the flow distribution within the structure and affect the magnitude of local pressure losses. The variant with a wall thickness of 0.7 mm exhibited more favorable hydraulic characteristics at higher flow velocities, which may indicate a more suitable combination of flow cross-sectional area and flow-path arrangement compared with the other evaluated variants.

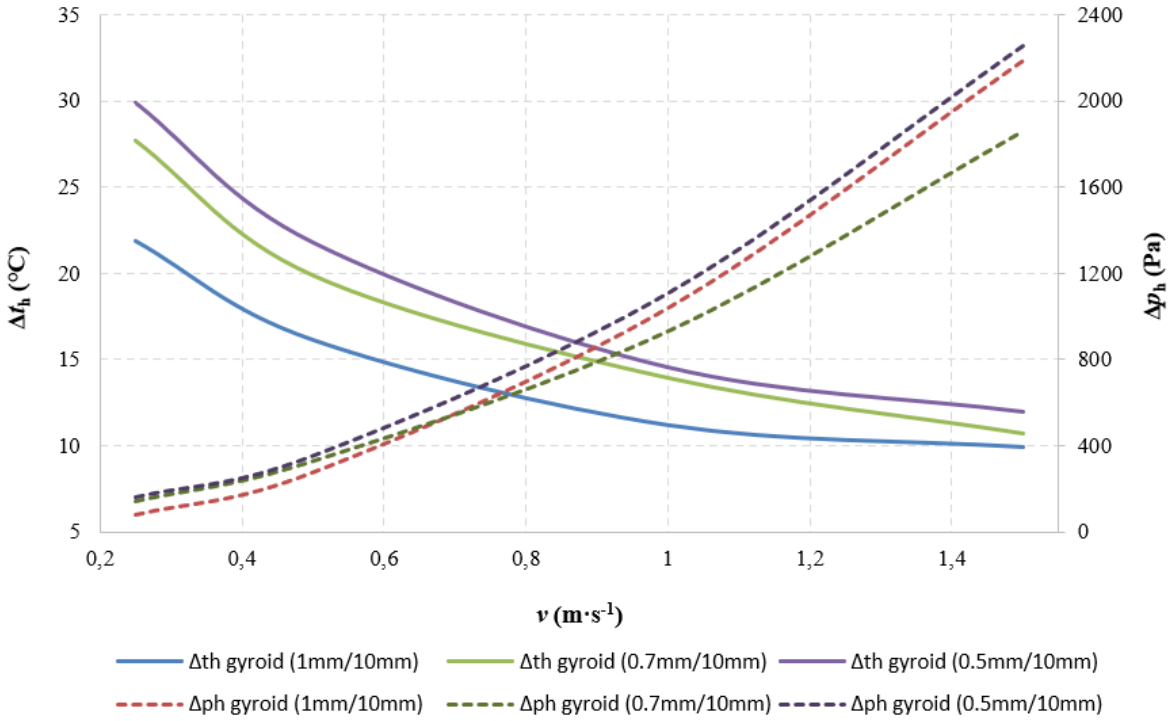


FIGURE 4: Comparison of pressure drop variation Δp_h and temperature change Δt_h on the cooled side in relation to the fluid inlet velocity into the heat exchanger

Overall, the results indicate that increasing the flow velocity leads to an increase in the heat-transfer coefficient and subsequently in the transferred thermal power. However, this positive trend is accompanied by a pronounced increase in pressure losses. At higher flow velocities, from 1 to 1.5 $m \cdot s^{-1}$, the pressure losses reach critical values, which adversely affects the overall thermo-hydraulic efficiency of the device. When defining the optimal geometry, it was therefore necessary to evaluate heat transfer simultaneously with the hydraulic resistance of the structure.

The Gyroid structure was identified as the most suitable TPMS type for further design and optimization of the TPMS heat exchanger. It can be readily manufactured by additive manufacturing and provides smoothly curved channels without sharp transitions, which promote mixing and enhance heat transfer while maintaining pressure losses at an acceptable level.

When evaluating the individual gyroid structure variants, the assessment of the interplay between the heat transfer intensity and hydraulic resistance proved to be critical. Based on these criteria, the variant with a cell size of 10 mm and a wall thickness of 0.7 mm was selected as the final design suitable for experimental purposes and for assessing its suitability under real operating conditions. This variant represents an ideal compromise between high heat-transfer efficiency and acceptable pressure losses.

IV. CONCLUSION

The numerical simulation results showed that the characteristics of the proposed heat exchanger are strongly influenced not only by the TPMS structure type itself, but also by the choice of its geometric parameters and operating conditions. It was confirmed that increasing the flow velocity increases the heat-transfer coefficient and thermal power, while simultaneously causing a pronounced rise in pressure losses. Among the compared variants, the Gyroid structure with a wall thickness of 0.7 mm and a cell size of 10 mm was found to be the most advantageous. The numerical analysis clearly confirmed that the final geometry cannot be selected solely on the basis of maximizing heat transfer; instead, it must represent an optimization compromise between the intensity of heat transport between the media and the hydrodynamic losses of the device. The findings obtained in the presented research provide an appropriate methodological and design basis for follow-up studies. Further research should focus primarily on additive manufacturing of the proposed heat exchanger, its experimental verification, dimensional optimization for specific operating applications, and assessment of the long-term operational reliability of the proposed solution.

ACKNOWLEDGEMENTS

This work was supported by the Slovak Research and Development Agency under the Contract No. APVV-23-0266 and APVV-21-0274. It was further supported by the VEGA granting agency within Project No. 1/0587/25 and by the KEGA granting agency within Project No. 031TUKE-4/2025.

REFERENCES

[1] Blanquer, S., et al. (2017). Surface curvature in triply-periodic minimal surface architectures as a distinct design parameter in preparing advanced tissue engineering scaffolds. *Biofabrication*, *9*, 025001.

[2] Feng, J., et al. (2022). Triply periodic minimal surface (TPMS) porous structures: From multi-scale design, precise additive manufacturing to multidisciplinary applications. *International Journal of Extreme Manufacturing*, *4*(2), 022001.

[3] Dutkowski, K., et al. (2022). Review of the state-of-the-art uses of minimal surfaces in heat transfer. *Energies*, *15*(21), 1-25.

[4] nTop, Inc. (2023). *Thermal management guide: Heat exchanger design for additive manufacturing*. nTop. https://ntopology.com

[5] Vlahinos, M., & O'Hara, R. (2020). *Unlocking advanced heat exchanger design and simulation with nTop platform and ANSYS CFX* [Technical report]. https://revolutioninsimulation.org

[6] E-konstruktér. (2015). *Hustota a specifická hmotnost vody*. https://e-konstrukter.cz/prakticka-informace/hustota-a-specificka-hmotnost-vody

[7] Kizek, J. (n.d.). *Vybrané vlastnosti vody*. https://jan.kizek.website.tuke.sk/tabulky/vlastnosti%20vody.htm

[8] Shah, R. K., & Sekulić, D. P. (2003). *Fundamentals of heat exchanger design*. John Wiley & Sons.